Functional Properties of the Purified Na^+-Dependent Citrate Carrier of *Klebsiella pneumoniae*: Evidence for Asymmetric Orientation of the Carrier Protein in Proteoliposomes

Klaas Martinus Pos and Peter Dimroth*

Mikrobiologisches Institut, Eidgenössische Technische Hochschule, ETH-Zentrum, Schmelzbergstrasse 7, CH-8092 Zürich, Switzerland

Received July 14, 1995; Revised Manuscript Received October 16, 1995[⊗]

ABSTRACT: The sodium-ion-dependent citrate carrier of *Klebsiella pneumoniae* (CitS) was purified and reconstituted into liposomes to investigate the properties of this transport system without interference from other proteins. Citrate uptake was an electroneutral process, where ΔpNa^+ and/or ΔpH are driving forces. $\Delta\psi$ was unable to stimulate citrate transport, either alone or in addition to the other driving forces. Sodium ions on the inside of the proteoliposomes stimulated the uptake of citrate, indicating that Na^+ ions recycle during the transport of citrate. CitS also performed Na^+ counterflow in the absence of citrate. The citrate carrier performed citrate/citrate counterflow but no heterologous antiport of citrate with one of the end products arising from the anaerobic citrate fermentation pathway (acetate, formate, or bicarbonate) in *K. pneumoniae*. Citrate counterflow kinetics revealed that CitS transports citrate according to a simultaneous type of mechanism. The K_m and K_i values revealed two binding sites for citrate: one with low and one with high affinity. This transport mode is in accord with an asymmetric organization of the carrier protein in proteoliposomes.

Klebsiella pneumoniae has the capacity to express at least three different citrate carriers that enable this enterobacterial species to grow on citrate under aerobic or anaerobic conditions (Schwarz & Oesterhelt, 1985). The genes for these citrate carriers were identified by screening a cosmid library of *K. pneumoniae* prepared in *Escherichia coli* (which usually exhibits a Cit^- phenotype)[1] for growth on citrate. In one of the three positive clones identified, the gene conferring the Cit^+ phenotype (*citH*) was apparently constitutively expressed under aerobic conditions. The DNA sequence of *citH* was determined and the gene product studied (van der Rest et al., 1990, 1991). It was concluded that CitH preferably transported one species of citrate ($HCit^{2-}$) in cotransport with three protons. The second clone which probably contains an inducible aerobic citrate transport system has not yet been characterized (Schwarz & Oesterhelt, 1985).

The third Cit^+ clone was able to grow on citrate not only aerobically, but also anaerobically. The cosmid conferring this property to *E. coli* harbors a cluster of genes that are specifically required for citrate fermentation and are believed to form a regulon. These include the genes for citrate lyase (*citDEF*), an oxaloacetate decarboxylase Na^+ pump (*oadGAB*), a Na^+-dependent citrate transporter (*citS*), and a two component regulatory system (*citAB*) (Bott et al., 1995). The DNA sequence of this entire region has recently been determined (Schwarz et al., 1988; Laussermair et al., 1989; Woehlke et al., 1992; van der Rest et al., 1992a; Bott & Dimroth, 1994; Bott et al., 1995). The *citS* gene encodes a highly hydrophobic protein with a predicted M_r of 47 531 and 12 putative membrane-spanning α-helices.

The properties of the Na^+-dependent citrate carrier (CitS) have been investigated in a reconstituted proteoliposomal system with the carrier protein derived from a Triton X-100 extract of *K. pneumoniae* membranes (Dimroth & Thomer, 1990) and with vesicles from CitS expressing *E. coli* cells (van der Rest et al., 1992a). In proteoliposomes containing CitS, citrate uptake with an imposed ΔpNa^+ as sole driving force was unaffected by the addition of valinomycin or FCCP (Dimroth & Thomer, 1990), suggesting an electroneutral Na^+−citrate symport mechanism. However, studies with membrane vesicles of transformed *E. coli* cells containing CitS (van der Rest et al., 1992a) seemed to indicate that citrate transport was mainly driven by ΔpH and to a lesser extent by $\Delta\psi$ and ΔpNa^+. The highest uptake rates were found when ΔpH, $\Delta\psi$, and ΔpNa^+ were imposed. These data suggested that citrate is translocated electrogenically across the membrane in symport with protons and sodium ions. The sodium/citrate stoichiometry was predicted to be 1 (van der Rest et al., 1992b). However, more recent studies on whole *E. coli* cells expressing CitS indicated a Na^+/citrate stoichiometry of 2 (Lolkema et al., 1994). Further studies indicated that $HCit^{2-}$ was probably the citrate species transported by CitS (van der Rest et al., 1992b).

* Author to whom correspondence should be addressed. Phone: (41) 1 632 33 21; Fax: (41) 1 632 11 48.

[⊗] Abstract published in *Advance ACS Abstracts,* January 1, 1996.

[1] Abbreviations: Cit, citrate; *citH*, gene for proton-dependent citrate transporter of *K. pneumoniae*; CitH, proton-dependent citrate carrier of *K. pneumoniae*; *citS*, gene for sodium-dependent citrate transporter of *K. pneumoniae*; CitS, sodium-dependent citrate carrier of *K. pneumoniae*; $CitS_{His}$, CitS with a N-terminally attached polyhistidine tail; DFP, diisopropyl fluorophosphate; dodecyl maltoside, dodecyl β-D-maltoside; FCCP, carbonyl cyanide *p*-(trifluoromethoxy)phenylhydrazone; IPTG, isopropyl β-D-thiogalactopyranoside; NTA, nitrilotriacetic acid; *oadGAB*, the genes for oxaloacetate decarboxylase of *K. pneumoniae*; *citDEF*, the genes for citrate lyase of *K. pneumoniae*; *citAB*, genes for a two component regulatory system in *K. pneumoniae*; ΔpH, pH gradient across the membrane; ΔpNa^+, chemical gradient of sodium ions across the membrane; $\Delta\psi$, electrical potential across the membrane; $\Delta\mu Na^+$, electrochemical gradient of sodium ions across the membrane.

0006-2960/96/0435-1018$12.00/0

Recently, we have purified CitS fusion proteins with a C-terminal biotin peptide or a N-terminal histidine tag by affinity chromatography (Pos et al., 1994). After reconstitution into liposomes, CitS catalyzed citrate uptake in response to ΔpNa^+. We have now extended these transport studies with the purified citrate carrier and show here that citrate transport is an electroneutral event driven by ΔpNa^+ and/or ΔpH but not by $\Delta\psi$. Evidence is also provided that the mechanism of citrate transport is more complex than anticipated: The citrate carrier transports citrate according to a sequential mechanism. Part of the Na^+ ions transported into the proteoliposomes together with citrate probably recycle during the translocation step. The results shown here lead to fundamentally new insights into the catalytic mechanism of citrate transport across the cytoplasmic membrane of *K. pneumoniae*.

EXPERIMENTAL PROCEDURES

Bacterial Strains and Plasmids. For plasmids pET-16b (Novagen, Madison, WI), $pCitS_{His}$, $pCitS_{His\text{-}2}$, and $pCitS_{His\text{-}3}$, the *Escherichia coli* strain BL21(DE3) or *E. coli* DH5α was used as host.

Media, Antibiotics, and Bacterial Growth. Luria broth (LB) and LB-agar were used for routine bacterial growth (Sambrook et al., 1989). Ampicillin was added at 100 μg/mL (Amp^{100}). Simmons' citrate agar (Simmons, 1926), supplemented with 4 μg/mL thiamine and Amp^{100}, was used to select for citrate utilizing clones.

Recombinant DNA Work and DNA Sequence Analysis. Routine work with recombinant DNA was performed according to established protocols (Sambrook et al., 1989). Sequence analysis was performed according to the dideoxynucleotide chain termination method (Sanger et al., 1977) using a Taq DyeDeoxy terminator cycle sequencing kit and the model 370A DNA sequencer from Applied Biosystems (Foster City, CA).

Construction of 10× His-Tagged $CitS_{His}$ Fusion. We recently reported the expression and purification of CitS fused with 6 histidine residues at its N-terminus (Pos et al., 1994). To increase the level of expression of CitS, the gene of the citrate carrier (*citS*) was recloned into another expression system (pET system, Novagen, Madison, WI). pFXa-2 (Pos et al., 1994) was restricted with *Bam*HI, and the resulting 1.3 kb fragment was cloned into a *Bam*HI restricted, dephosphorylated pET-16b vector to obtain $pCitS_{His\text{-}2}$. *E. coli* BL21(DE3) harboring $pCitS_{His\text{-}2}$ cannot express a functional His-tagged CitS protein because the inserted fragment was cloned out of frame relative to the vector derived start codon. Therefore, $pCitS_{His\text{-}2}$ was restricted with *Xho*I, the overhangs filled in a Klenow reaction, and religated to obtain $pCitS_{His\text{-}3}$. $pCitS_{His\text{-}3}$ conferred the cit^+ phenotype to *E. coli* BL21(DE3) under aerobic conditions. The DNA sequence of the fusion site was controlled by sequencing.

Expression of the Fusion Protein. *E. coli* BL21 (DE3)/$pCitS_{His\text{-}3}$ was grown overnight in 3 mL of LB Amp^{100} at 37 °C and 180 rpm. The cells were collected by centrifugation, resuspended in 1 mL of fresh LB medium, and used to inoculate 2 L of LB Amp^{100}. The bacteria were grown at 37 °C/180 rpm to an OD_{600nm} of 1.6 before harvest. Induction of the cells with IPTG in a range of 50−100 μM led to a modest growth inhibition that was not further investigated. About 5 g of wet packed cells were obtained.

Purification of the 10× His-Tagged CitS Fusion Protein. All sodium phosphate buffers used in this study were prepared from Na_2HPO_4 by adjusting the pH with HCl. "Sodium-free" phosphate buffers were prepared from phosphoric acid and KOH. $CitS_{His\text{-}3}$ was purified according to the protocol described earlier (Pos et al., 1994) with slight modifications: 5 g of *E. coli* BL21(DE3)/$pCitS_{His\text{-}3}$ cells (wet weight) were treated as described (Pos et al., 1994) to obtain 3 mL of Triton X-100 extract (30 mg of protein). The Triton X-100 extract was applied to a Ni^{2+}-NTA column (Qiagen) (3 mL bed volume) equilibrated with buffer A (20 mM K_2HPO_4, 40 mM NaCl, 20 mM potassium citrate, 10 mM imidazole, 10% (v/v) glycerol (as stabilizer), 0.1% (w/v) dodecyl maltoside, adjusted to pH 7.8 with HCl). The column was successively washed with 20 mL of buffer A and 20 mL of buffer B (buffer A containing 100 mM imidazole, adjusted to pH 6.0 with HCl) to remove unbound proteins. $CitS_{His\text{-}3}$ ($CitS_{His}$) was specifically eluted with buffer C (buffer A containing 500 mM imidazole adjusted to pH 7.0 with HCl). The yield was 1.5−3 mg of apparently pure protein, indicating that at least 5 −10% of the protein present in the Triton X-100 extract was $CitS_{His}$.

Incorporation of the Purified Fusion Protein into Liposomes. To form liposomes, a suspension of 28 mg of soybean phosphatidylcholine (type II S, Sigma) in 900 or 950 μL of reconstitution buffer (see below) was vigorously agitated with a vortex mixer for 3 min and afterward sonicated for 2 × 30 s at 40 W with a microtip. The purified fusion protein (50 or 100 μL, 20−50 μg of protein) or 50−100 μL of buffer C (as control) was added to the preformed liposomes, and the mixture was kept for 15 min on ice with occasional shaking. Undesired salts (citrate, NaCl) added with the protein were subsequently removed by chromatography of 1 mL of the reconstitution mixture on a NAP-10 column (Pharmacia) in reconstitution buffer (see below). The first three drops containing proteoliposomes (detected by turbidity) were discarded, and the next 0.5 mL was collected, frozen in liquid nitrogen, thawed in a water/ice bath, and sonicated for 1 × 5 s at 40 W with a microtip. In some occasions, the proteoliposomes were concentrated by centrifugation (180000*g*, 50 min) and resuspended in reconstitution buffer (see below) to yield a final volume of 100 μL.

Citrate Transport. Citrate transport was initiated by diluting 2 μL of proteoliposomes in a defined reconstitution buffer (see below) into 98 μL of assay buffer containing 12 μM [1,5-^{14}C]citrate (NEN-Du Pont or Amersham; 100−250 cpm/pmol). The mixture was briefly blended on a vortex mixer and incubated in a 25 °C waterbath. After various times, the transport of citrate was terminated by adding 900 μL of ice-cold 0.1 M LiCl or KCl followed by rapid filtration through 0.22 μm GSTF filters (Ø 25 mm, Millipore). The filters were washed once with 1 mL of ice-cold 0.1 M LiCl or KCl and placed into scintillation vials. After addition of 4 mL of scintillation fluid (Beckman, Ready-safe) the entrapped [1,5-^{14}C]citrate was determined by liquid scintillation counting. Experimental values were corrected for zero-time controls. Therefore, the proteoliposomes (2 μL) were positioned on the wall of a tube containing 98 μL of assay buffer. Subsequently, 900 μL of ice-cold 0.1 M LiCl or KCl was added and the mixture was rapidly filtered as described above.

(i) Determination of V_{max} and K_m for Citrate. Proteoliposomes (2 μL) prepared in 49 mM potassium phosphate

containing 1 mM sodium phosphate, pH 6.0 (ΔpNa^+-driven uptake), or in 50 mM potassium phosphate, pH 7.5 (($\Delta pNa^+ + \Delta pH$)-driven uptake), were diluted into 98 μL of 50 mM sodium phosphate, pH 6.0 ($\Delta pNa^+ = -100$ mV, ($\Delta pNa^+ + \Delta pH$) = -206.5 mV (for $[Na^+_{in}] = 1$ mM)), containing various amounts of [1,5-^{14}C]citrate (1.5−24 μM, 170−240 cpm/pmol). From the kinetics of citrate transport, initial velocities were obtained. The data were transformed using the Michaelis−Menten equation and plotted according to Lineweaver−Burk. The kinetic constants were derived from these plots.

(ii) Citrate Counterflow. For determination of the kinetic mechanism of citrate exchange, proteoliposomes were prepared in 25 mM potassium phosphate containing 25 mM sodium phosphate, pH 6.3, with different internal potassium citrate concentrations ranging from 0.5 to 20 mM. After freezing/thawing/sonication, 250 μL of these proteoliposomes was applied on an NAP-10 column equilibrated in 25 mM potassium phosphate containing 25 mM sodium phosphate, pH 6.3. The first nine turbid drops (approximately 250 μL) were collected (from a total turbid volume of 750 μL). Control experiments where the internal pool of citrate was labeled had shown that almost no citrate leaks out of the proteoliposomes within 10 min at 25 °C (data not shown). Therefore, this approach was sufficiently satisfactory to perform the following kinetic experiments: One microliter of [1,5-^{14}C]citrate (120 μM−1.2 mM, 154−170 cpm/pmol) was added to 20 μL of proteoliposomes which were previously incubated for 1 min at 25 °C. This mixture was briefly mixed on a vortex mixer. After 5 s, the reaction was terminated by addition of 900 μL of ice-cold 0.1 M LiCl and immediately filtered (see above). The values obtained after liquid scintillation counting were processed using the Michaelis−Menten equation and used in Lineweaver−Burk plots from which secondary plots were constructed according to Cleland (1970).

(iii) Citrate Transport with Artificial Driving Forces. Proteoliposomes (2 μL) prepared in 50 mM potassium phosphate, pH 7.5, containing 5 mM Na_2SO_4 were diluted into 98 μL of (a) 50 mM sodium phosphate, pH 7.5, to create a ΔpNa^+ of −59 mV; (b) 50 mM potassium phosphate, pH 6.3, containing 5 mM Na_2SO_4 to create a ΔpH of −71 mV; (c) 50 mM sodium phosphate, pH 6.0, to create a $\Delta pNa^+ + \Delta pH$ of −147.5 mV. Proteoliposomes (2 μL) prepared in 50 mM potassium phosphate, pH 6.3, containing 5 mM Na_2SO_4, were diluted into 98 μL of 50 mM Tris−phosphate, pH 6.3, containing 5 mM Na_2SO_4 and 0.8 μM valinomycin to create a $\Delta\psi$ of −100 mV. All buffers used for dilution of the proteoliposomes contained 12 μM [1,5-^{14}C]citrate (170−240 cpm/pmol). Citrate uptake into the proteoliposomes was subsequently determined as described above.

Na^+ Counterflow. Proteoliposomes A were prepared in 50 mM sodium phosphate, pH 7.5; proteoliposomes B (control) were prepared in 50 mM potassium phosphate, pH 7.5. As a control, proteoliposomes A were also reconstituted with $CitS_{His}$, which was previously boiled for 5 min. Proteoliposomes A or B (10 μL) were diluted into 190 μL of 50 mM potassium phosphate, pH 7.5, or into 190 μL of 47.5 mM potassium phosphate, pH 7.5, containing 2.5 mM sodium phosphate, pH 7.5, respectively. Carrier free ^{22}NaCl was added to the incubation mixtures to create a specific activity of $^{22}Na^+$ of 880 cpm/nmol. After various times, samples (200 μL) were passed over small columns of Dowex 50, K^+ (about 0.5 −1 mL bed volume), to adsorb the external $^{22}Na^+$. The resin was washed twice with 300 μL of ice-cold 50 mM Tris−phosphate, pH 7.5. The radioactivity entrapped inside the proteoliposomes was afterward determined by γ-scintillation counting. The values obtained from the control experiments (unspecific Na^+ uptake) were substracted from the values obtained for Na^+ counterflow.

Protein Determination. Protein was determined according to the method of Bradford (1976) using as a standard bovine serum albumin (BSA) that was dissolved in the same buffer as the samples.

RESULTS

Construction of $pCitS_{His\text{-}3}$. We recently described the expression of the Na^+-dependent citrate carrier (CitS) fused at the N-terminus with 6 histidine residues in *E. coli* and its subsequent purification by Ni^{2+}−NTA affinity chromatography (Pos et al., 1994). The expression and purification have now been improved by recloning the *citS* gene fused to 10 histidine residues at the N-terminus using the pET expression system as described under Experimental Procedures. With this system the level of expression of $CitS_{His}$ increased to 5−10% of the proteins present in the Triton X-100 extract of the bacterial membranes. The citrate carrier was subsequently purified by the Ni^{2+}−NTA affinity column to apparent homogeneity (SDS−PAGE). The yield was 1−1.5 mg of pure protein/L of the recombinant *E. coli* culture. The purified citrate carrier was reconstituted into liposomes by a freeze/thaw/sonication procedure, and the derived proteoliposomes were used for all of the transport studies described below.

Driving Forces for Citrate Uptake Are ΔpNa^+ and ΔpH, but Not $\Delta\psi$. The kinetics of citrate transport into proteoliposomes containing purified CitS in response to ΔpNa^+, ΔpH, $\Delta\psi$, or combinations of these parameters were performed to elucidate the driving forces for this transport. The results in Figure 1 show a large stimulation of citrate uptake by applying ΔpNa^+ or ΔpH and further stimulation of the transport if the two driving forces are applied simultaneously. Citrate was not accumulated above background levels (in the absence of ΔpH and ΔpNa^+), however, by imposing a $\Delta\psi$ of −100 mV, nor was $\Delta\psi$ of any effect on ΔpNa^+- or ΔpH-driven citrate transport. We conclude from these data that citrate transport by CitS is an electroneutral symport with Na^+ and H^+. These results confirm in part earlier reports on citrate transport with proteoliposomes prepared with crude membrane extracts of *K. pneumoniae* (Dimroth & Thomer, 1990). The conclusion from previous studies that citrate transport is an electrogenic event and therefore driven by $\Delta\psi$, however, is not in accord with our data (van der Rest et al., 1992a).

Is an Antiport Mechanism Involved in Citrate Uptake? Secondary transporters may use symport with an ion like H^+ or Na^+ or antiport with a metabolic end product to accumulate a specific substrate within the cell. The anaerobic degradation of citrate by *K. pneumoniae* produces acetate, bicarbonate, and formate as metabolic end products. The gradient of one or several of these products from the inside to the outside of the cell could therefore be used to drive citrate uptake by an antiport mechanism. If proteoliposomes were loaded with 10 mM each of potassium acetate and $KHCO_3$ and subsequently diluted into buffer without acetate

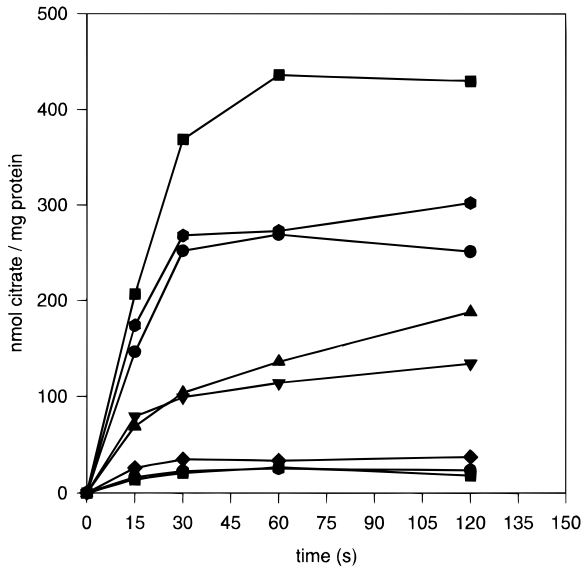

FIGURE 1: Effect of ΔpNa^+, ΔpH, or $\Delta\psi$ on citrate uptake into proteoliposomes containing $CitS_{His}$. The proteoliposomes for each assay were prepared as described in the Experimental Procedures. The uptake of [1,5-^{14}C]citrate was initiated by diluting 2 μL of proteoliposomes into 98 μL of assay buffer containing 12 μM [1,5-^{14}C]citrate. Imposed driving forces: ΔpNa^+ (−59 mV, pH 6.0, ⬢), $\Delta pNa^+ + \Delta\psi$ (−59 mV + (−100 mV) = −159 mV, pH 6.0, ● upper symbols), ΔpH (−53 mV, 10 mM $Na^+_{in=out}$, ▲), ΔpH (−53 mV, 10 mM $Na^+_{in=out}$, + valinomycin (0.8 μM), ▼), $\Delta\psi$ (−100 mV, pH 6.3, 10 mM $Na^+_{in=out}$, ■ lower symbols), ΔpH + nigericin (20 μM) (10 mM $Na^+_{in=out}$, ♦), no gradient (pH 6.3, 10 mM $Na^+_{in=out}$, ● lower symbols), $\Delta pH + \Delta pNa^+$ (−59 mV + (−88.5 mV) = −147.5 mV, 100 mM Na^+_{out}; 10 mM Na^+_{in}, ■ upper symbols).

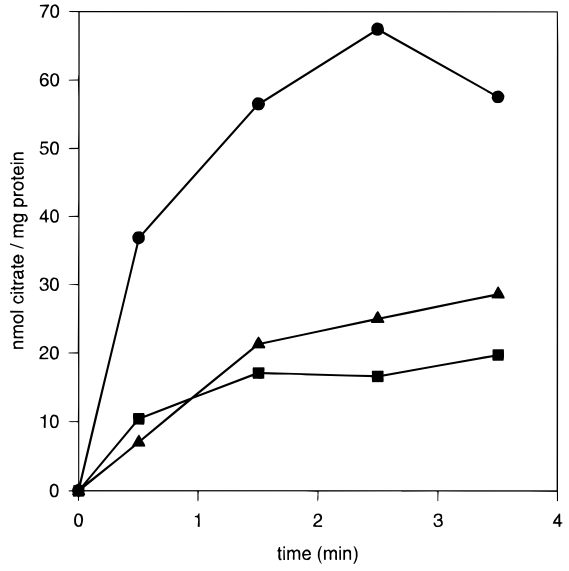

FIGURE 2: Effect of acetate and bicarbonate on citrate uptake into proteoliposomes containing purified $CitS_{His}$. The proteoliposomes were prepared in 50 mM potassium phosphate, pH 6.0, containing 10 mM potassium acetate, 10 mM $KHCO_3$, and 1 mM NaCl (●) or in 50 mM potassium phosphate, pH 6.0, containing 1 mM NaCl (▲). Proteoliposomes were diluted into 490 μL of 50 mM potassium phosphate, pH 6.0, containing 1 mM NaCl and 12 μM [1,5-^{14}C]-citrate (170 cpm/pmol). In a control experiment (■), proteoliposomes (prepared in 50 mM potassium phosphate, pH 6.0, containing 10 mM potassium acetate, 10 mM $KHCO_3$, and 1 mM NaCl) were preincubated for 2 min at 25 °C with 600 nM nigericin before dilution. At given times, 100 μL samples were taken and diluted into 900 μL of ice-cold LiCl and filtered as described under Experimental Procedures.

and bicarbonate containing [1,5-^{14}C]citrate, the tricarboxylic acid was accumulated more rapidly and to a higher level than with unloaded proteoliposomes (Figure 2). Similar results were also obtained by loading the proteoliposomes with acetate and formate, or with acetate, formate and bicarbonate (not shown). These results are not conclusive evidence for an antiport mechanism, however, because diffusion of these acids from the inside to the outside will create a ΔpH (acid outside) which could contribute to the driving force for citrate uptake. In the presence of nigericin which dissipates a ΔpH by K^+/H^+ exchange, the kinetics of citrate uptake into the loaded and unloaded proteoliposomes were the same. These results are not compatible with citrate/acetate, formate, and/or bicarbonate antiport, but are in accord with a citrate/H^+ symport mechanism. Further evidence against an antiport mechanism was the failure of acetate, bicarbonate, or formate added to the outside to inhibit ΔpNa^+-driven citrate uptake into the proteoliposomes containing purified $CitS_{His}$. Furthermore, internal citrate was without effect on the uptake of [1-^{14}C]acetate into proteoliposomes under various assay conditions (data not shown).

Dependence of Citrate Uptake on ΔpNa^+ Imposed by Constant Internal and Varying External Na^+ Concentrations and Vice Versa. The initial velocity of citrate uptake was studied in response to ΔpNa^+ between −59 and −100 mV. In one series of experiments, the internal Na^+ concentration was kept at 2 mM and the external Na^+ concentration was varied between 20 and 100 mM. Under these conditions, the citrate transport velocity increased continuously with increasing ΔpNa^+ (Figure 3). Different results were obtained, however, by generating the same set of ΔpNa^+ values

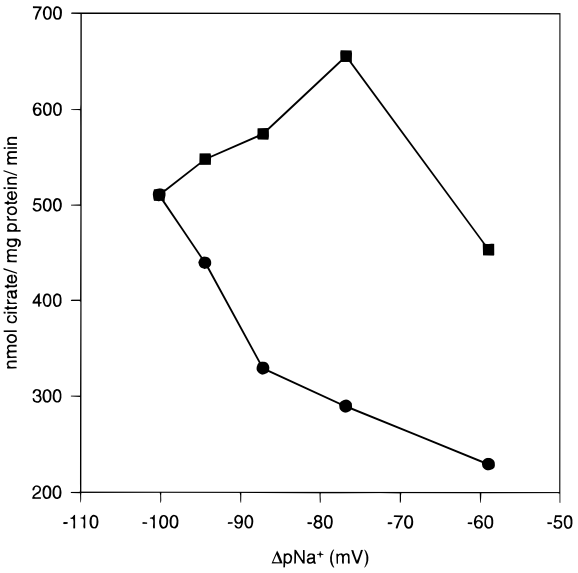

FIGURE 3: Effect of ΔpNa^+ at constant internal and varying external Na^+ concentrations (●) and vice versa (■) on initial [1,5-^{14}C]citrate uptake into $CitS_{His}$ liposomes. The proteoliposomes were prepared in the presence of potassium phosphate, pH 7.5, with addition of (A) 1 mM sodium phosphate (●), or (B) 1, 1.25, 1.67, 2.5, or 5 mM sodium phosphate (■) (total phosphate concentration: 50 mM). The proteoliposomes (2 μL) were diluted into 98 μL of (A) 50, 40, 30, 20, or 10 mM sodium phosphate buffer, pH 7.5 (●), or (B) 50 mM sodium phosphate, pH 7.5 (■). Dilution buffers contained 12 μM [1,5-^{14}C]citrate (170 cpm/pmol).

through differences of the internal Na^+ concentration at a fixed external Na^+ concentration of 100 mM. Under these conditions, citrate transport increased on decreasing ΔpNa^+

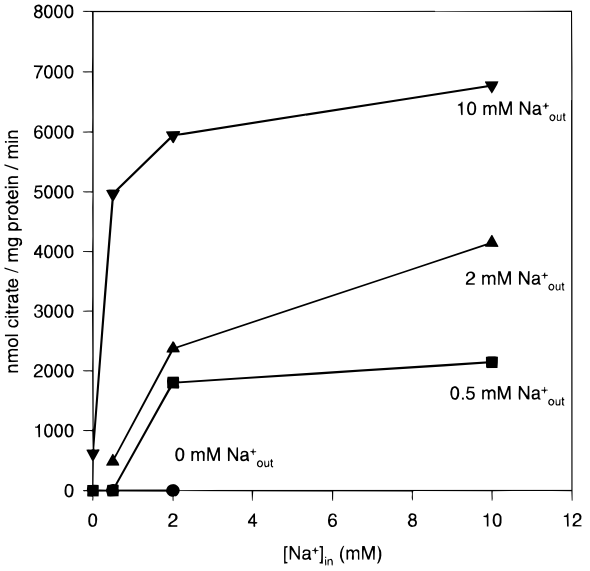

FIGURE 4: Na^+ dependence of citrate counterflow activity at pH 6.8. Proteoliposomes were prepared in 50 mM potassium phosphate, pH 6.8, containing 5 mM potassium citrate and various concentrations of sodium chloride, as indicated. The proteoliposomes (5 μL) were diluted 1:20 into 50 mM potassium phosphate buffer, pH 6.8, containing 0 (●), 0.5 (■), 2 (▲), and 10 mM sodium chloride (▼) and 12 μM [1,5-^{14}C]citrate (8600−9500 cpm/nmol). The initial values were obtained from 10 s measurements.

from −100 to −77 mV and started to drop only on further decreasing ΔpNa^+ to −59 mV. It is also remarkable that the velocity of citrate transport was significantly higher if identical ΔpNa^+ values of less than −100 mV were generated by increasing the internal Na^+ concentrations rather than by decreasing the external Na^+ concentrations. These results thus indicate that the transport of citrate depends not only on ΔpNa^+ but also on internal Na^+ ions, suggesting an important role of these internal Na^+ ions in the citrate transport mechanism.

Effect of Internal and External Na^+ Concentration on Citrate Counterflow. The finding that ΔpNa^+-driven citrate uptake was stimulated by internal Na^+ ions prompted us to investigate the effect of internal and external Na^+ ion concentration on citrate counterflow. The results in Figure 4 indicate no counterflow activity in the absence of both internal and external Na^+ ions, as expected. No counterflow activity was also observed with no Na^+ addition to the outside and up to 2 mM Na^+ on the inside or with 0.5 mM Na^+ on both sides of the membrane. A very low counterflow activity was seen if 0.5 mM Na^+ and 2 mM Na^+ were present on the inside and the outside, respectively, or if Na^+ was not added to the inside at 10 mM Na^+ on the outside. The highest counterflow activity was observed if 10 mM Na^+ was present on both sides of the membrane. Decreasing the internal Na^+ concentration to 2 and 0.5 mM at a fixed external Na^+ concentration of 10 mM reduced the counterflow rate only by about 25%, while decreasing the external Na^+ concentration correspondingly at a fixed internal Na^+ concentration of 10 mM resulted in a more severe reduction of counterflow activity by about 70%.

In summary, these results indicate a requirement for Na^+ on both sides of the membrane for citrate counterflow activity. Furthermore, an asymmetric feature of the citrate carrier is evident from the more significant response of citrate counterflow on varying external than on varying internal Na^+ concentrations. As the movement of labeled citrate (262 μM) was stimulated at least 16-fold by 5 mM internal citrate (our counterflow conditions) under all experimental conditions shown in Figure 4, an interference of the counterflow data by citrate uptake can be excluded.

Bireactant Initial Velocity Studies: Evidence for Asymmetric Orientation of the Citrate Carrier Protein. The counterexchange of citrate catalyzed by CitS can be described as a two substrate reaction involving different association/dissociation and catalytic steps. The sequence of these steps follows one of two basically different bireactant mechanisms, either the ping-pong or the simultaneous mechanism. A clear distinction between these mechanisms can be made from the kinetic pattern obtained in studies of the antiport velocity as a function of both internal and external citrate concentrations (Cleland, 1970; Dierks et al., 1988; Bisaccia et al., 1993; Stappen & Krämer, 1993, 1994; Indiveri et al., 1993). The results of a bireactant initial velocity study of citrate/citrate homoexchange are shown in Figure 5A,B. The Lineweaver−Burk plots derived from five different external and six different internal citrate concentrations show an intersecting pattern of straight lines. This intersecting pattern demonstrates that the antiport reaction follows a simultaneous type of mechanism, implying that both countersubstrate molecules have to form a ternary complex with the carrier protein prior to the translocation step. The transport rate was greatly stimulated when rising the external or internal citrate concentration, as can be recognized from the effect on the apparent V_{max}. Intriguingly, variation of the citrate concentration in one compartment also markedly influenced the apparent transport affinity of citrate in the other compartment ($K_m(cit_{ex})$: 24.7−92.1 μM and $K_m(cit_{in})$: 2.4−6 mM). Further analysis of these data in secondary plots, where slopes and ordinate intercepts of Figure 5A,B were plotted against the reciprocal concentration of the substrate in the opposite compartment, are shown in Figure 5C,D. From the linear relations obtained, the K_m values at infinite citrate concentration in the respective opposite compartment could be extrapolated. These values were 140.5 μM for external citrate and 13.5 mM for internal citrate. The results are summarized in Table 1. From the secondary plots also, the K_i values representing the dissociation constants of the binary carrier substrate complexes in a simultaneous mechanism were derived ($K_i(cit_{ex})$: 20.4 μM and $K_i(cit_{in})$: 1.96 mM). From the relationship $K_i(cit_{ex})K_m(cit_{in}) = (K_m(cit_{ex})K_i(cit_{in})$ (in this case: $(K_i(cit_{ex})K_m(cit_{in}))/((K_m(cit_{ex})K_i(cit_{in})) \approx 1$), a particular case of simultaneous mechanism can be distinguished, namely, a rapid equilibration random mechanism (although the ratio K_m/K_i for both internal citrate and external citrate is 6.8, this is not proof for distinguishing the type of transport mechanism (Cleland, 1970)). Interestingly, the K_m values for external citrate in ΔpNa^+-driven citrate uptake are near or below the K_m value of citrate/citrate exchange with 0.5 mM citrate at the inside (see Table 1). Although these values were obtained at pH 6.0 (counterflow studies were performed at pH 6.3), it shows that when citrate is lacking on the opposite side of the transport direction, the K_m values are in close relationship with the idea that internal citrate is decreasing the affinity for external citrate. The K_m values are also indicating that the citrate carrier protein has an asymmetric orientation in the membrane. We consider the possibility that CitS acts as a dimeric protein during transport. The V_{max} derived from the secondary plots was

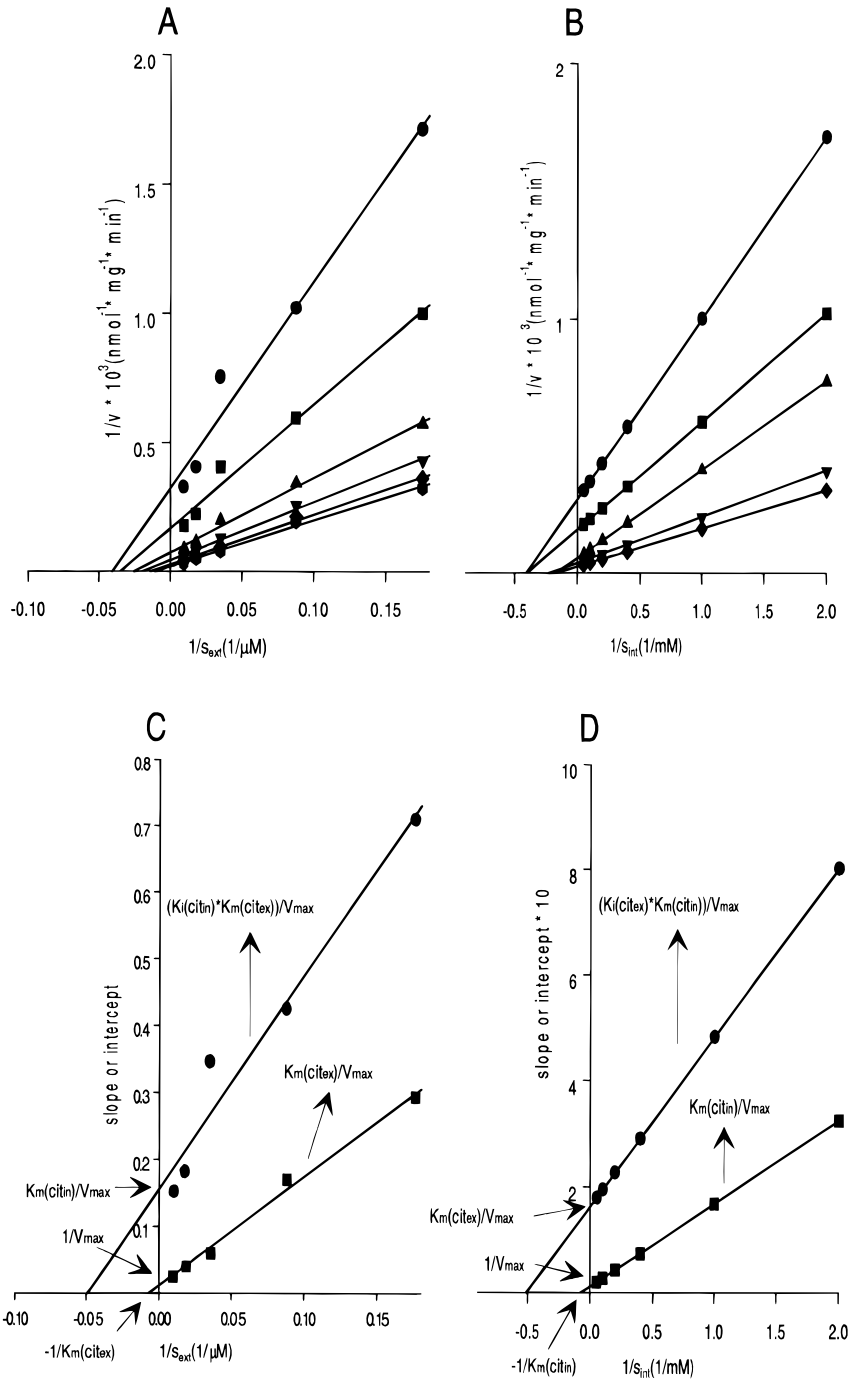

FIGURE 5: Lineweaver−Burk plots showing citrate/citrate counterflow activity as a function of six internal citrate concentrations (A: 0.5 (●), 1 (■), 2.5 (▲), 5 (▼), 10 (♦), 20 mM (⬢)) and five external citrate concentrations (B: 5.7 (●), 11.4 (■), 28.6 (▲), 57.1 (▼), 109.1 μM (◆)). Based on the calculated intercepts (■) and slopes (●), secondary plots were made (C, D). The calculated K_i values were 20.4 μM for external citrate and 1.96 mM for internal citrate. The calculated K_m values for internal and external citrate at infinite concentrations of citrate at the opposite compartment were 13.5 mM and 140.5 μM, respectively. The calculated V_{max} values for infinitive concentration of internal and external citrate are 8.6 μmol/(mg·min).

8.6 μmol/(min·mg of protein). The turnover number of CitS (dimer) in citrate/citrate exchange is thus about 137 s^{-1}.

In summary, the results could indicate that the citrate carrier functions as a dimer (but by no means a definite proof), where each monomer has its own binding site for citrate. Citrate is apparently bound with high affinity to one of these sites and will be transported in response to ΔpNa^+ without occupation of the second citrate binding site. High concentrations of citrate in this compartment, on the other hand, will lead to its binding to a low affinity site, leading to the exchange of external and internal citrate. The absolute requirement for Na^+ also indicates that Na^+ binding site(s) must be occupied in addition to the citrate binding sites to achieve either of these activities of CitS. The stimulation obtained by adding increasing amounts of Na^+ on the internal compartment during ΔpNa^+-driven citrate transport also indicates that Na^+ sites directed toward the internal compartment should be occupied before transport of citrate occurs.

Na^+ Counterflow. All data on the mechanism of CitS are consistent with a Na^+−citrate cotransport. Direct demonstration of Na^+ uptake together with citrate into protoliposomes using the isotope $^{22}Na^+$ was not possible, however,

Table 1: Determination of K_m Values for Citrate Transport in either Uptake (ΔpNa^+-Driven or ($\Delta pNa^+ + \Delta pH$)-Driven) or Counterflow Mode[a]

condition	cit_{in} (mM)	$K_m(cit_{ex})$ (μM)	pH
ΔpNa^+	0	13.9 (9.5)	6.0
$\Delta pNa^+ + \Delta pH$	0	13.0 (8.9)	6.0
counterflow	0.5	24.7 (13.5)	6.3
	1	28.7 (15.7)	
	2.5	39.2 (21.4)	
	5	52.9 (28.9)	
	10	71.5 (39.1)	
	20	92.1 (50.3)	
	∞	140.5 (76.8)	
condition	cit_{ex} (μM)	$K_m(cit_{in})$ (mM)	pH
counterflow	5.7	2.4 (1.3)	6.3
	11.4	2.5 (1.4)	
	28.6	5.9 (3.2)	
	57.1	4.5 (2.5)	
	109.1	6.0 (3.3)	
	∞	13.5 (7.4)	

[a] The ΔpNa^+ was about −100 mV and $\Delta pNa^+ + \Delta pH$ was about −206.5 mV. The values in brackets represent the K_m values for the citrate species $Hcit^{2-}$ which is the species believed to be transported. pK values of citrate: p$K_a(1) = 3.128$, p$K_a(2) = 4.76$, p$K_a(3) = 6.396$.

due to technical reasons (the specific activity of $^{22}Na^+$ that could be obtained with reasonable amounts of radioactivity was below the detection level after transport due to the high Na^+ concentrations required).

The exchange mode of the carrier and its Na^+ dependence indicate that internal and external Na^+ ions are also exchanged in this process. Furthermore, the requirement of internal Na^+ ions for ΔpNa^+-driven citrate uptake suggests a turnover of Na^+ ions between the external and internal compartment. It was conceivable therefore, that this turnover of Na^+ did also occur in the absence of citrate. Proteoliposomes containing CitS were therefore loaded with 100 mM Na^+ salts and diluted 20-fold into buffer to which carrier-free $^{22}NaCl$ was added to yield 5 mM $^{22}Na^+$ (specific activity: 880 cpm/nmol) on the outside. The ΔpNa^+ generated by this procedure was +77 mV (from the inside to the outside). The results of Figure 6 show that $^{22}Na^+$ was taken up by these proteoliposomes. $^{22}Na^+$ uptake was also observed if no Na^+ was contained within the proteoliposomes or if these were formed with denatured CitS, but this uptake was about 50% slower. After subtracting this background movement of Na^+ ions, the rate of Na^+ counterflow was calculated to be 158 nmol/(min·mg of protein). This means that Na^+ counterflow is about 545 times slower than citrate counterflow.

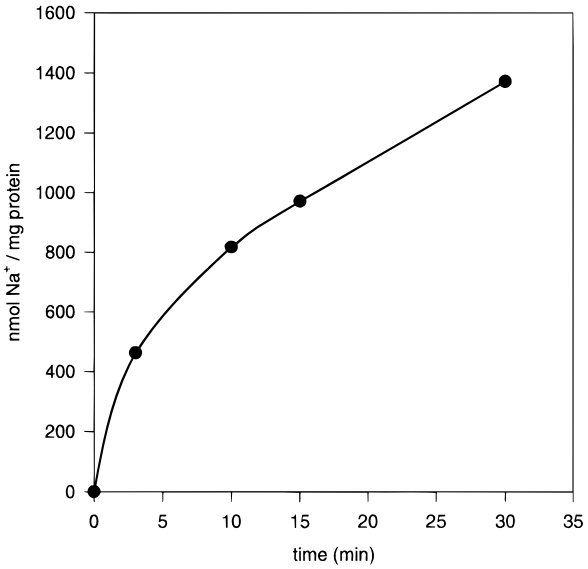

FIGURE 6: $^{22}Na^+$ counterflow into $CitS_{His}$ containing proteoliposomes loaded with 100 mM Na^+. Counterflow was initiated by diluting 10 μL of these proteoliposomes into 190 μL of Na^+-free buffer that contained $^{22}NaCl$ (carrier-free) to generate a ΔpNa^+ of about 77 mV from the inside to the outside (●). The values were corrected for unspecific uptake of Na^+ as described under Experimental Procedures.

DISCUSSION

The Na^+-dependent citrate carrier from *K. pneumoniae* (CitS) transports citrate from the outside to the inside of the cell in symport with Na^+ ions. We show here that no heterologous antiport between citrate and one of the end products of citrate fermentation (acetate, formate, or bicarbonate) is facilitated by CitS. Driving forces for citrate uptake are ΔpNa^+ and ΔpH, but not $\Delta\psi$ because the electrical potential has no effect on citrate uptake. The electroneutral transport has important consequences regarding the stoichiometry of the Na^+/H^+/citrate cotransport. It implies that two of these cations are transported with citrate because $Hcit^{2-}$ was shown to be the species transported by CitS (van der Rest et al., 1992b). Results from this laboratory are in accord with this observation. The findings that Na^+ ions are obligatory for citrate uptake and that ΔpH (and ΔpNa^+) are driving forces therefore indicate that the transport stoichiometry is 1 Na^+ plus 1 H^+ per $Hcit^{2-}$. This conception deviates, however, from previous reports which favor a stoichiometry of 2 Na^+ plus 1 H^+ per $Hcit^{2-}$ (Lolkema et al., 1994). The conclusion was based on the finding of an electrogenic citrate transport and on kinetic data which indicated the interaction of (at least) two Na^+ binding sites in a cooperative manner during transport. An important result of the present paper is the observation that the rate of ΔpNa^+-driven citrate transport is greatly enhanced by internal Na^+ ions, although the driving force becomes significantly reduced. The best explanation for this observation is binding of Na^+ to the carrier from both sides of the membrane during the course of citrate transport. Explicitly, we assume that the citrate binding site oriented outward must be occupied with $Hcit^{2-}$ and 2 Na^+ to initiate a conformational change and release the ions to the inside. We further assume that reorientation of the (empty) citrate binding site requires binding of 1 Na^+ (and OH^-, see below) from the inside and release of these Na^+ ions to the outside. The essentials of this concept are shown in:

$$Hcit^{2-}{}_{out} + 2Na^+{}_{out} + 1Na^+{}_{in} + 1OH^-{}_{in} \rightarrow Hcit^{2-}{}_{in} + 2Na^+{}_{in} + 1Na^+{}_{out} + 1OH^-{}_{out} \quad (1)$$

The model is in accord with ΔpNa^+ and ΔpH being driving forces because the overall stoichiometry would be a cotransport of $Hcit^{2-}$ with 1 Na^+ and 1 H^+. We cannot discriminate from our data whether H^+ is transported together with citrate or whether OH^- is (formally) transported in the opposite direction. We slightly favor the second possibility because both parts of the cycle would be electroneutral whereas in the first case the uptake of positive charge in the first half

of the cycle would be compensated by extrusion of positive charge in the second half. The model is further in accord with the electroneutral transport of citrate and with the cooperation of (at least) $2Na^+$ binding sites (Lolkema et al., 1994), and it gives a reasonable explanation for the enhancement of ΔpNa^+-driven citrate uptake by internal Na^+ ions (this work).

In case of the phosphate carrier from bovine heart, mitochondria evidence was obtained that discriminate between H^+/phosphate symport and OH^-/phosphate antiport in favor of the latter (Stappen & Krämer, 1994). This carrier functions as a dimer and transports inorganic phosphate (P_i) electroneutrally from the cytoplasm into the mitochondrial matrix. The carrier protein also catalyzes P_i/P_i exchange, and the kinetic mechanism was elucidated for both exchange and uptake mode. The results clearly showed that the phosphate carrier catalyzed phosphate transport according to a simultaneous mechanism; i.e., binding sites for phosphate and OH^- are exposed by the dimeric molecule to the outside and the inside, respectively, and must be simultaneously occupied to accomplish the translocation step. The function of dimeric carrier proteins in a simultaneous mechanism is common for the mitochondrial carrier protein family which includes, e.g., the tricarboxylate carrier (Bisaccia et al., 1993).

Since some of the properties of these mitochondrial carriers seemed to resemble those of CitS, we studied the mechanism of CitS by citrate/citrate counterflow experiments. Such studies can be used to discriminate between two basically different transport mechanisms, the simultaneous mechanism (see above) or the ping-pong mechanism, where a substrate binds from one side of the membrane, becomes translocated, and is released to the other side before the reaction proceeds in the reverse direction. Quite surprisingly, our results clearly indicate that citrate/citrate exchange follows a simultaneous mechanism. Thus, two citrate binding sites exposed to the two different sites of the membrane must be occupied before the translocation can proceed and the substrates can be released to the opposite sides of the membrane. An intriguing observation of these studies was that the binding sites exposed by CitS to the two opposite sides of the membrane were of highly different affinities for citrate, one with high affinity (micromolar range) and one with low affinity (millimolar range). In the counterflow mode (high citrate concentration on the inside and low citrate concentration on the outside) only those carrier proteins with the high affinity site exposed to the outside are expected to be active. The influence of the citrate concentration in one compartment on the affinity of citrate in the other compartment is additional evidence for an exposure of two citrate binding sites by one CitS molecule to the two different membrane sides. The relationship between the kinetic constants follows the equation $K_i(cit_{in})K_m(cit_{ex}) = K_i(cit_{ex})K_m(cit_{in})$. This relationship is characteristic for a rapid equilibrium random simultaneous mechanism (Cleland, 1970). The simultaneous mechanism demonstrated for CitS is quite common among the mitochondrial carrier proteins, but has not been shown yet for a prokaryotic carrier. Typical examples are the lactose permease of *E. coli* or the arginine/ornithine antiporter from *Lactococcus lactis* which function by a ping-pong mechanism (Garcia et al., 1983; Driessen et al., 1989). Furthermore, most prokaryotic carrier proteins were shown (Costello et al., 1987; Ambudkar et al., 1990) or are believed to be catalytically active monomers. We have recently purified a fusion protein of CitS with a biotinylation domain by avidin−Sepharose affinity chromatography. Surprisingly, two equally stained bands (apparent M_r 50 000 and 33 000) were observed after SDS−PAGE and silver staining. Both polypeptides had identical N-termini. Only the polypeptide with apparent M_r 50 000 was biotinylated. The non-biotinylated polypeptide of apparent M_r 30 000 had the same mobility as unmodified CitS. The non-biotinylated protein, which was present in excess in the detergent extract of the membranes, could therefore only be retained on the affinity column by forming a complex with the biotinylated CitS specimen. The same results were obtained if the chromatography was performed in the presence of Triton X-100, dodecyl maltoside, or Brij 58. These data have therefore been taken as (preliminary) evidence for an oligomeric most likely dimeric organization of CitS (Pos et al., 1994). This observation itself is of course insufficient to prove that a dimer is the catalytically active form of the carrier. The simultaneous presence of two citrate binding sites on CitS would, however, be more easily explained if its active species is a dimer. The dependence of citrate counterflow on Na^+ on both sides of the membrane indicates that Na^+ ions are cotransported with citrate also in this transport mode. A high external Na^+ concentration was more important than a high internal Na^+ concentration to achieve high counterflow activity. This result suggests that not only the binding sites of a CitS molecule for citrate but also those for Na^+ are oriented asymmetrically within the membrane.

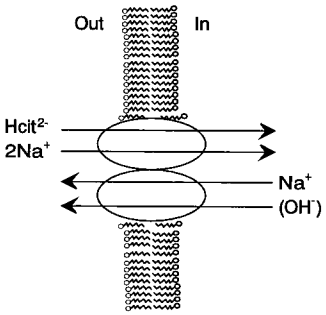

FIGURE 7: Model for citrate transport by *K. pneumoniae*. The dimeric citrate carrier (CitS) is represented by the the ovals drawn in the the figurative membrane. The *net* transport of citrate ($Hcit^{2-}$) occurs electroneutrally in symport with 1 Na^+ and in antiport with a hydroxyl ion. Note that the anticipated transport of a hydroxyl ion is mere formalism and could more likely proceed by abstraction of a proton from a protonated amino acide side chain on one side of the membrane (in) and reprotonation of this group on the other side of the membrane (out).

Based on the data described here and in part on data described elsewhere (van der Rest et al., 1992ab; Lolkema et al., 1994), a model for citrate uptake is proposed that is shown in Figure 7. In this model we assume that the catalytically active species of CitS is a dimer. The high affinity binding site of the carrier is exposed to the outside where it is occupied with $Hcit^{2-}$. The electrical charge of the citrate dianion is neutralized after the additional binding of 2 Na^+ ions from the outside to the same monomer of CitS. According to the simultaneous mechanism, the binding sites of the other monomer that are exposed to the inside must be filled before the translocation step can occur. We assume binding of a hydroxyl ion to the anion binding site, which then allows only 1 Na^+ to bind from the inside of this monomer of CitS, again resulting in compensating the electrical charge of the bound ions. After the dimer of CitS

has been occupied from both sides with the ions specified, a conformational change leads to the reorientation of the binding sites toward the other compartment where the bound ions are subsequently released. Formally, the overall transport can be written as:

$$Hcit^{2-}{}_{out} + 2Na^{+}{}_{out} + Na^{+}{}_{in} + OH^{-}{}_{in} \rightarrow Hcit^{2-}{}_{in} + Na^{+}{}_{in} + OH^{-}{}_{out} \quad (2)$$

Please note that the anticipated transport of a hydroxyl ion is mere formalism and could more likely proceed by abstraction of a proton from a protonated amino acid side chain on one side of the membrane and reprotonation of this group on the other side of the membrane. In the presence of high internal citrate concentrations, $Hcit^{2-}$ may bind instead of OH^- at the binding site of the internally oriented monomer. After the additional binding of 2 Na^+ to this monomer, citrate counterflow can be catalyzed.

The model also has to account for regenerating a high affinity citrate binding site on the outside once the substrate has been released in order to accomplish continuous citrate uptake. Either the empty CitS has to perform another conformational change that brings it back into its original state or the conformational change that reorients the binding sites on each monomer is accompanied with a change in their binding affinities. The originally high affinity binding sites for citrate exposed to the outside may become a low affinity binding site for citrate (and simultaneously an OH^- binding site) after exposure to the inside, and the originally low affinity citrate binding site on the other monomer may become a high affinity site after its exposure to the outside.

The model further predicts that 2 Na^+ ions are bound if the anion binding site is occupied with $Hcit^{2-}$ whereas only 1 Na^+ is bound if this site is occupied with OH^-. One possible explanation could be the presence of 1 Na^+ binding site at each oppositely exposed monomer that is independent from the occupation of the anion site with $Hcit^{2-}$ or OH^-. The anion site could be provided by a positively charged amino acid side chain (Arg or Lys). This could form a salt bridge with one of the carboxylate groups of citrate, and the second carboxylate group of $Hcit^{2-}$ could be part of another Na^+ binding site of the carrier. Binding of OH^- instead of $Hcit^{2-}$ would deprotonate the positively charged amino acid side chain, and the second Na^+ binding site would not be created.

From the physiological point of view, uptake of $Hcit^{2-}$ with 1 Na^+ and 1 H^+ is easier to synchronize with the other Na^+ translocating proteins present in *K. pneumoniae* fermenting citrate. Citrate is converted to oxaloacetate in this organism, and this is decarboxylated to pyruvate by the oxaloacetate decarboxylase Na^+ pump. While in the absence of $\Delta\mu Na^+$ the ratio of Na^+ transported to oxaloacetate decarboxylated is about 2, Na^+ ion pumping against a $\Delta\mu Na^+$ leads to Na^+ to oxaloactetate stoichiometries that are clearly lower than 2 and more likely closer to 1 (Dimroth & Thomer, 1993). The amount of Na^+ ions pumped from the oxaloacetate decarboxylase would thus not suffice to accomplish citrate uptake if the Na^+ to citrate stoichiometry would be 2 rather than 1. One has also to take into account that part of the Na^+ ions exported by oxaloacetate decarboxylase recycle by the Na^+-dependent NADH:ubiquinone oxidoreductase during NADH synthesis for biosynthetic purposes by $\Delta\mu Na^+$-driven reversed electron transfer (Pfenninger-Li & Dimroth, 1992).

ACKNOWLEDGMENT

We would like to thank Prof. R. Krämer (Jülich) for critically reading the manuscript.

REFERENCES

Ambudkar, S. V., Anantharam, V., & Maloney, P. C. (1990) *J. Biol. Chem. 265*, 12287−12292.
Bisaccia, F., De Palma, A., Dierks, T., Krämer, R., & Palmieri, F. (1993) *Biochim. Biophys. Acta 1142*, 139−145.
Bott, M., & Dimroth, P. (1994) *Mol. Microbiol. 14*, 347−356.
Bott, M., Meyer, M., & Dimroth, P. (1995) *Mol. Microbiol.* (in press).
Bradford, M. M. (1976) *Anal. Biochem. 72*, 248−254.
Cleland, W. W. (1970) in *The Enzymes* (Boyer, P. D., Ed.) Vol. 2, pp 1−65, Academic Press, New York.
Costello, M. J., Escaig, J., Matsushita, K., Viitanen, P. V., Menick, D. R., & Kaback, H. R. (1987) *J. Biol. Chem. 262*, 17072−17082.
Dierks, T., & Krämer, R. (1988) *Biochim. Biophys. Acta 937*, 112−126.
Dierks, T., Riemer, E., & Krämer, R. (1988) *Biochim. Biophys. Acta 943*, 231−244.
Dimroth, P., & Thomer, A. (1990) *J. Biol. Chem. 265*, 7721−7724.
Dimroth, P., & Thomer, A. (1993) *Biochemistry 32*, 1734−1739.
Driessen, A. J. M., Molenaar, D., & Konings, W. N. (1989) *J. Biol. Chem. 264*, 10361−10370.
Garcia, M. L., Viitanen, P., Foster, D. L., & Kaback, H. R. (1983) *Biochemistry 22*, 2524−2531.
Indiveri, C., Prezioso, G., Dierks, T., Krämer, R., & Palmieri, F. (1993) *Biochim. Biophys. Acta 1143*, 310−318.
Laussermair, E., Schwarz, E., Oesterhelt, D., Reinke, H., Beyreuther, K., & Dimroth, P. (1989) *J. Biol. Chem. 264*, 14710−14715.
Lolkema, J. S., Enequist, H., & van der Rest, M. E. (1994) *Eur. J. Biochem. 220*, 469−475.
Pfenninger-Li, X. D., & Dimroth, P. (1992) *Mol. Microbiol. 6*, 1943−1948.
Pos, K. M., Bott, M., & Dimroth, P. (1994) *FEBS Lett. 347*, 37−41.
Sambrook, J., Fritsch, E. F., & Maniatis, T. (1989) *Molecular Cloning: A Laboratory Manual*, 2nd ed., Cold Spring Harbor Laboratory, Cold Spring Harbor, NY.
Sanger, F., Nicklen, S., & Coulson, A. R. (1977) *Proc. Natl. Acad. Sci. U.S.A. 74*, 5463−5467.
Schwarz, E., & Oesterhelt, D. (1985) *EMBO J. 4*, 1599−1603.
Schwarz, E., Oesterhelt, D., Reinke, H., Beyreuther, K., & Dimroth, P. (1988) *J. Biol. Chem. 263*, 9640−9645.
Simmons, J. S. (1926) *J. Infect. Dis. 39*, 209−241.
Stappen, R., & Krämer, R. (1993) *Biochim. Biophys. Acta 1149*, 40−48.
Stappen, R., & Krämer, R. (1994) *J. Biol. Chem. 269*, 11240−11246.
van der Rest, M. E., Schwarz, E., Oesterhelt, D., & Konings, W. N. (1990) *Eur. J. Biochem. 189*, 401−407.
van der Rest, M. E., Abee, T., Molenaar, D., & Konings, W. N. (1991) *Eur. J. Biochem. 195*, 71−77.
van der Rest, M. E., Siewe, R. M., Abee, T., Schwarz, E., Oesterhelt, D., & Konings, W. N. (1992a) *J. Biol. Chem. 267*, 8971−8976.
van der Rest, M. E., Molenaar, D., & Konings, W. N. (1992b) *J. Bacteriol. 174*, 4893−4898.
Woehlke, G., Laussermair, E., Schwarz, E., Oesterhelt, D., Reinke, H., Beyreuther, K., & Dimroth, P. (1992) *J. Biol. Chem. 267*, 22804−22805.

BI951609T